doi:10.4149/neo_2021_210511N642

Determination of biological behavior of solitary fibrous tumors: correlation of expression of *Ki-67*, *TPX2* and *TERT* mRNA subunit level and *NAB2-STAT6* fusion compared to morphological aspects of SFTs

Lenka KRSKOVÁ[1,*], Igor ODINTSOV[1,2], Ondřej FABIÁN[1,3,4], Petra HROUDOVÁ[1,5], Marcela MRHALOVÁ[1]

[1]*Department of Pathology and Molecular Medicine, 2nd Faculty of Medicine, Charles University and University Hospital Motol, Prague, Czech Republic;* [2]*Department of Pathology, Memorial Sloan Kettering Cancer Center, New York, United States;* [3]*Department of Pathology and Molecular Medicine, 3rd Faculty of Medicine, Charles University and Thomayer University Hospital, Prague, Czech Republic;* [4]*Clinical and Transplant Pathology Centre, Institute for Clinical and Experimental Medicine, Prague, Czech Republic;* [5]*Department of Pathology, Hospital Ceske Budejovice, Ceske Budejovice, Czech Republic*

**Correspondence: lenka.krskova@lfmotol.cuni.cz*

Received May 11, 2021 / Accepted August 2, 2021

We present a retrospective study of 65 cases of solitary fibrous tumors (SFTs) of several localizations including the most common site of origin in the pleura and lungs. SFTs are mesenchymal fibroblastic tumors with an unpredictable biological potential ranging from benign to malignant. We investigated morphologic characteristics, proliferation activity evaluated by immunohistochemical expression of Ki-67 antigen, and the existence of NAB2-STAT6 fusion gene together with Ki-67, TPX2, and TERT mRNA expression levels. The aim was to define relationships between proliferation activity and biological potential and progression of the disease. We measured Ki-67, TPX2, and TERT mRNA levels using quantitative real-time reverse transcription PCR (RQ-RT-PCR). We observed a significant association between increased Ki-67 and TERT mRNA levels and the SFTs with malignant potential. Also, we investigated the effect of TERT promoter mutation on telomerase activation and patient outcome in our SFT cohort. We verified that TERT promoter mutation was frequent (36.6%) and present in a majority of malignant SFTs and SFTs with uncertain biological behavior. TERT promoter mutation alone predicted the disease recurrence.

Key words: solitary fibrous tumors (SFTs), NAB2-STAT6, proliferation markers, biological behavior, prognosis, TERT

A solitary fibrous tumor (SFT) is an uncommon neoplasm of the pleural and extrapleural site of origin formed by cells with fibroblastic features [1–3]. This tumor exhibits a spectrum of biological behavior and can occur at any age with the peak in the sixth and seventh decade of life [1, 3].

A typical immunoprofile of the tumor cells is positivity of CD34 (90–95%), EMA (Epithelial membrane antigen), BCL2 (B-cell lymphoma 2), and α-SMA (Alpha-Smooth Muscle Actin). In some of the malignant and dedifferentiated tumors, a loss of CD34 expression was observed [4–6]. Immunohistochemistry of STAT6 (Signal transducer and activator of transcription 6), especially by monoclonal anti-STAT6 antibody, is useful for the diagnosis of SFT [7–9]. Focal positivity for S100 protein, cytokeratins, or desmin might be seen as well [1, 3, 4, 10, 11].

The prognosis of these tumors is generally uncertain. Most cases are benign. However, their behavior can be unpredictable and even the benign variants may reoccur many years after total resection. Histological appearance, cell proliferation, and especially mitotic counts are for now the best predictable factor of further tumor behavior. Infiltrative growth pattern, necrosis, cell pleomorphic, and high proliferation activity should catch the attention [4, 12]. Lesions located in the mediastinum, retroperitoneum, abdomen, and meanings tend to behave more aggressively than those located in the soft tissue of the limbs [1]. Tumor size over 10 cm in diameter and positive surgical margins show a poorer prognosis [4].

Recently, massive parallel sequencing studies on solitary fibrous tumors have enabled the discovery of an intrachromosomal inversion-derived gene fusion, which juxtaposes the *NGFI-A* binding protein 2 (*NAB2*) gene on 12q13 and signal transducer and activator of transcription 6 (*STAT6*) gene on 12q13 [13–15]. The chimeric *NAB2-STAT6* fusion

transcript exhibits highly variable breakpoints across 5´exons of *NAB2* gene and 3´exons of *STAT6* gene.

In the present work, we evaluated the proliferation activity and prognosis of SFTs by investigating the activity of several molecules. We selected molecular markers which are important regulators of the cell cycle: *Ki-67, TPX2* (Microtubule Nucleation Factor), and a marker that is associated with the mechanism of cellular senescence – enzyme telomerase, specifically *TERT* telomerase catalytic subunit (TERT).

Ki-67 is a proliferation-associated nuclear antigen expressed by proliferating cells in all phases of the active cell cycle (G1, S, G2, and M phase). This antigen provides information about the proportion of the active cells in the cell cycle [16].

Another molecular marker, TPX2 is a microtubule-associated protein homolog. It plays an important role in mitotic spindle formation, and the segregation of chromosomes during cell division [17, 18]. TPX2 is expressed exclusively in the proliferating cells in the S, G2, and M phases of the cell cycle and its activity accurately corresponds to the proliferation activity of cells.

TERT is a frequently used marker, which is associated with the mechanism of cellular senescence. Telomeres protect the chromosomes from DNA degradation, end-to-end fusions, rearrangements, and chromosomal losses [19, 20]. The telomerase activity in human cancer was first demonstrated by Kim [21], and it has been detected in a wide variety of human malignancies implicating that the telomerase activity may play a role in the tumorigenic process [22]. This enzyme with a complex regulatory mechanism consists of three major components: RNA telomerase component (hTERC), telomerase-associated protein (TEP1), and telomerase catalytic subunit (TERT) [23]. *TERT* mRNA expression was shown to be most closely linked to telomerase activity [24].

Recurrent hot-spot mutations in *TERT* promoter have been reported in various types of tumors. In several tumor types, *TERT* promoter mutations are associated with poor clinical outcomes. Two hot-spot mutations, C228T and C250T, create novel binding sites for E-twenty-six (ETS) transcription factors, resulting in a maximum 4- to 5-fold increase in the induction of the *TERT* gene [25]. Importantly, *TERT* promoter mutations are associated with a worse clinical outcome in most studies further highlighting the role of telomerase activation in tumor progression and recurrence [26]. Noteworthy, some tumors without *TERT* promoter mutation may express *TERT* suggesting that the presence of additional mechanisms is necessary for telomerase activation.

In the current study, we investigated a possible impact of *NAB2-STAT6* fusion variants on clinicopathological features of SFTs and also investigated a possible impact of mRNA level of *Ki-67*, *TPX2,* and *TERT*. Also, we investigated the effect of *TERT* promoter mutation on telomerase activation and the biological behavior of SFTs.

Patients and methods

Patients and clinical data. We performed a retrospective study of 74 samples from 65 patients with solitary fibrous tumors diagnosed at the Department of Pathology and Molecular Medicine of the Faculty Hospital Motol, Prague, within the years 2006 and 2019.

All pathologic slides were reviewed independently by pathologists for the presence of pleomorphism, nuclear atypia, necrosis, hypercellularity, and the mitotic count per 10 high-power fields (HPFs).

After that, an immunohistochemical assessment of 74 tissue samples, from 65 patients was performed and analyzed for *Ki-67*, *TPX2* expression, *TERT* promoter mutations, and TERT expression. The range of those patients with SFT included 37 women and 28 men. The youngest patient was 21 years old, the oldest 86 (median 60 years at diagnosis). The most common site of origin was the pleura and lungs (37 patients, 57%).

Morphology and immunohistochemistry. For further examination, we used material of 74 cases of SFT. Histological sections were stained by Hematoxylin and Eosin for evaluation of morphology and for the mitotic count. Consequently, the proteins expression (CD34, BCL2, CD99, STAT6, and Ki-67) was investigated by immunohistochemistry (IHC). Immunohistochemistry was performed on formalin-fixed paraffin-embedded biopsy specimens. Representative 3 μm thick sections of the diagnostic biopsy and/or recurrent samples were used for immunohistochemistry.

After dewaxing and rehydration, heat-induced epitope retrieval was performed by heating in buffers pH 6 or pH 9 (specified in the Supplementary Table S1) in a water bath. Endogenous enzymatic activity was blocked by hydrogen peroxide in phosphate-buffered saline. Incubation at 4 °C overnight with primary antibodies followed (brands, clones, and used dilutions are summarized in the Supplementary Table S1). Detection was performed using a one-step polymeric, non-Biotin, Fab micropolymer detection system (Bio SB) based on peroxidase and 3,3´-diaminobenzidine reaction.

The cut-off for Ki-67 immunohistochemistry was 0–5% for benign tumors, 5–10% for uncertain, and more than 10% for malignant SFTs.

Detection of NAB2-STAT6 fusion transcript. Seventy-four samples from 65 patients of previously diagnosed SFTs for which frozen or FFPE (formalin-fixed, paraffin-embedded tissue) material were available, were examined for *NAB2-STAT6* fusion, the mRNA expression of proliferative markers, and *TERT* promoter mutation. Reverse transcription-polymerase chain reaction (RT-PCR) was performed on FFPE samples (58) except for 16 cases in which fresh frozen tumor tissue was available. Total RNA was extracted from fresh frozen material using TRIzol (Invitrogen, Ltd., Carlsbad, CA, USA) and from formalin-fixed, paraffin-embedded sections using High Pure RNA Paraffin

Kit (Roche Diagnostic, Mannheim, Germany) following the manufacturer's instructions for total mRNA isolation.

The complementary DNA (cDNA) was synthesized by reverse transcription using 1 μg of total RNA and primed using random hexamers and 50 units of MMLV Reverse Transcriptase (Invitrogen) according to the manufacturer's instructions. RT-PCR was performed using 2× PCRBIO HS Taq Mix Red (PCR Biosystems Ltd., London, UK) with primers located in *NAB2* exons 2 to 6 and reverse primers positioned in *STAT6* exons 2 to 20 (Supplementary Table 2). Amplification of a 208 bp amplicon of the *ABL* house-keeping gene was used to confirm the presence of intact and amplifiable cDNA. All detected *NAB2-STAT6* fusion variants were confirmed by Sanger sequencing. Direct Sanger sequencing was performed using Big Dye Terminator v 3.1 chemistry (Life Technologies) and an ABI PRISM 3130 genetic analyzer (Applied Biosystems). Results were analyzed using Chromas lite 2.01 (Technelysium, Pty Ltd, Brisbane, Australia) and the BLASTn Alignment tool (NIH, Bethesda, MD, USA) to compare the PCR product sequence to the *NAB2* and *STAT6* nucleotide sequences.

Quantitative real-time reverse transcription PCR (RQ-RT-PCR) of the proliferative markers and TERT. RQ-RT-PCR analyses were performed using LightCycler 480 detection system (Roche Diagnostic, Mannheim, Germany). The assessment of the expression levels of *Ki-67, TPX2,* and *TERT* catalytic subunit transcript was accomplished using the Universal Probe Library software system for Human (Roche Applied Science, Indianapolis, IN, USA). RQ-RT-PCR for housekeeping gene *β2-microglobulin* (*B2M*) using hydrolyzation probe was utilized to evaluate the amount and amplifiability of cDNA. The primers were designed as reported by Bijwaard et al. [27].

The sequences of the primers and probes are listed in Supplementary Table 2. Reaction conditions were as follows: reaction mixture comprised FastStart TaqMan Probe Master Mix (Roche Diagnostic, Mannheim, Germany), 500 nM of each sense and antisense primers, 100 nM of LNA probe and 1 μl cDNA in a final volume of 20 μl. The reaction was started with incubation at 50 °C for 2 min, initial denaturation at 95 °C for 10 min, followed by 50 PCR cycles: 95 °C for 20 s, and 60 °C for 1 min.

Detection of *Ki-67, TPX2, TERT,* and *B2M* copy numbers was performed according to a standard curve method. Consequent plasmid calibrators of each gene were used for standard curves construction.

All analyses were performed in duplicates and the mean value was taken for further calculations. Normalized expression of *Ki-67, TPX2, TERT* transcripts were calculated as a ratio between the expression levels of the marker and *B2M* housekeeping gene expression levels.

The TERT promoter mutation. The genomic DNA was extracted from each formalin-fixed, paraffin-embedded tissue block using QIAamp DNA FFPE Tissue Kit (Qiagen, Germany) When isolating DNA, the most representative tissue blocks, containing the maximum percentage of tumor tissue were selected. The *TERT* promoter region mutations were examined using polymerase chain reaction (PCR), followed by direct sequencing. Amplification was performed using 2× PCRBIO HS Taq Mix Red (PCR Biosystems Ltd., London, UK) with primers located in the promoter region. The PCR products were electrophoresed in a 1.5% agarose gel and were recovered using the Gel DNA Fragments Extraction Kit (Geneaid, Taiwan). Direct Sanger sequencing was performed using Big Dye Terminator v 3.1 chemistry (Life Technologies) and an ABI PRISM 3130 genetic analyzer (Applied Biosystems). Results were analyzed using Chromas lite 2.01 (Technelysium, Pty Ltd, Brisbane, Australia).

Fluorescence in situ hybridization (FISH) analysis. Detection of the copy numbers of *TERT* gene signals was evaluated by FISH using ZytoLight® SPEC TERT/5q31 Dual Color probes mixture (Z-2091-200, ZytoVision) on histological sections from formalin-fixed and paraffin-embedded tissues. Signals were counted in at least 100 tumor cells nuclei. The results were evaluated using a fluorescence microscope.

Statistical analysis. For the statistical analysis, we used JMP IN 5.1. software (SAS Institute, Cary, NC, USA). Kruskal-Wallis nonparametric test was applied to assess differences in the mRNA levels of the molecular markers within SFTs and benign/malignant potential of SFTs. p-values <0.05 were considered statistically significant.

Results

According to WHO classification [3] all 65 patients with solitary fibrous tumors were divided into groups of benign (31 cases; 47.7%), malignant (12 cases; 18.5%), and with uncertain biological behavior (22 cases; 33.8%). All cases were evaluated by considering tumor localization, microscopic appearance, mitotic rate, presence of cellular atypia, necrosis, and proliferation activity measured by Ki-67 expression.

Nowadays due to accessible data 48 patients are disease-free – 28 with originally benign, 4 with malignant, and 16 with SFT with uncertain biological behavior. In seven patients with malignant SFT and six patients with SFT with uncertain biological behavior, a progression of the disease was observed.

One patient with malignant SFT died because of a disease progression and metastatic dissemination 4 years after primary diagnosis and two patients died because of other diseases than SFT.

Immunohistochemistry. Expressions of CD34, CD99, BCL2, STAT6, and Ki-67 molecules were evaluated by immunohistochemistry. STAT6 was positive in all stained cases (66 cases, 100%, Figure 1).

The proliferation index measured by Ki-67 expression of benign tumors was maximally 3%. The proliferation activity in tumors with uncertain biological behavior spreads between 2% and 10% (median 4). The proliferation activity in malig-

nant tumors rated from 5–70% (median 15) of tumor cells and higher mitotic activity was also seen.

The Ki-67 staining achieved statistical significance when compared to the malignant and benign biological behavior of tumors ($p<0.0001$), when compared malignant and uncertain behavior ($p=0.0012$), and also in uncertain and benign biological behavior ($p<0.0001$). Tumors with higher proliferative activity also had a greater tendency to relapse ($p<0.0001$). Spearman correlation coefficient for the number of mitoses and Ki-67 staining was $p<0.0001$.

The median and/or count of mitosis per 10 HPFs was 1 (range 0–26). Mitosis count per HPF was significantly higher in malignant (median 8, range 0–26) compared with SFTs with uncertain biological behavior (median 1, range 0–6, $p=0.0014$) or benign (median 0, range 0–2, $p=0.0100$).

RT-PCR. Results of the molecular analysis are summarized in Supplementary Table S3. *NAB2-STAT6* fusion transcript was found in 63/74 cases (85%) of amplifiable samples and in 57/65 patients with SFT (87.7%). Most fusions occurred between *NAB2* exon 4 and *STAT6* exon 2 (32/55, 58%). All of them were detected in the lung or pleura SFTs, except 1 case where meningeal SFT was diagnosed. This patient with meningeal SFT had two fusions: *NAB2* exon 4 and *STAT6* exon 2, and *NAB2* exon 5 and *STAT6* exon 2. Fourteen patients had the fusion of exon 6 of *NAB2* with exon 16, intron 16, or exon 17 of the *STAT6* gene. In 3 tumor samples, no *NAB2-STAT6* fusion was detected because of the quality of isolated RNA from FFPEs (negativity of control house-keeping gene *ABL*), and in 5 tumor samples, no *NAB2-STAT6* fusion was detected, but the quality of isolated RNA was good.

Of the 60 molecularly examined SFTs for which prognostic data were available, 13 patients had local recurrence and/or metastasis (21.6%). We did not observe any statistical difference in the frequency of local recurrence and

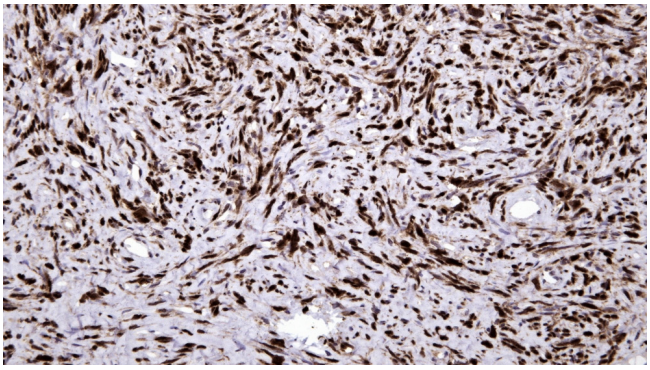

Figure 1. Immunohistochemical staining of STAT6 showing nuclear positivity, original magnification ×200.

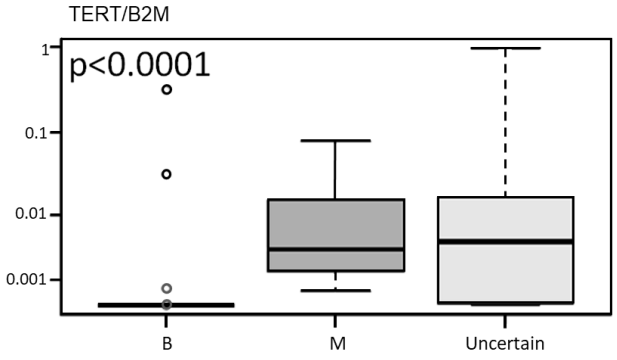

Figure 2. Box plot graph demonstrates the distribution of *TERT* mRNA expression levels on benign (B), malignant (M), and uncertain SFTs. SFTs with malignant and/or uncertain behavior expressed a significantly higher level than benign (Kruskal-Wallis Test, $p<0.0001$). Boxes represent values between the 25th and 75th percentile with the median, whiskers represent the 10th and 90th percentile, and outlying values are represented by dots. Vertical line TERT/B2M in copies/µl; horizontal line, SFTs with benign, uncertain, and malignant potential.

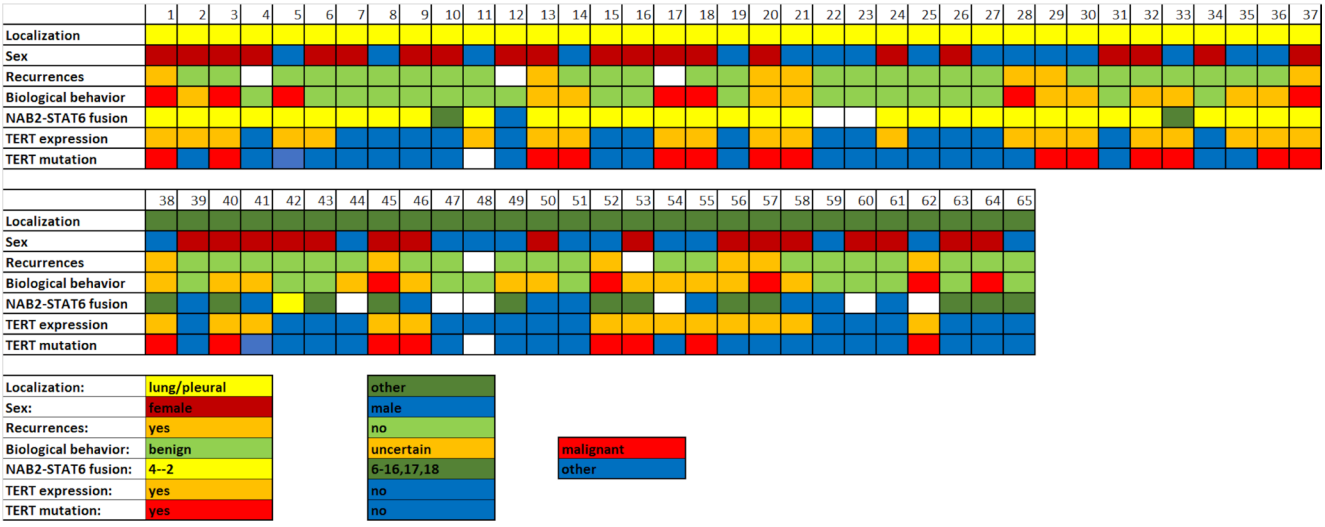

Figure 3. OncoPlot demonstrating genetic and clinical features of patients with solitary fibrous tumors.

the type of fusion transcript *NAB2/STAT6* or localization of the primary tumor.

RQ-RT-PCR of proliferative markers and TERT. 74 samples available for molecular testing from 65 patients with histological diagnosis of SFT were analyzed.

The level mRNA for housekeeping gene *β2-microglobulin* varied in paraffin-embedded samples (median 3.4×10^4) and in frozen samples (median 2.22×10^5). The real-time RT-PCR assay was validated using 5 paraffin-embedded samples tested previously on cryosections. We observed a similar ratio of all proliferative markers/*β2-microglobulin* in both paraffin-embedded samples and cryosections.

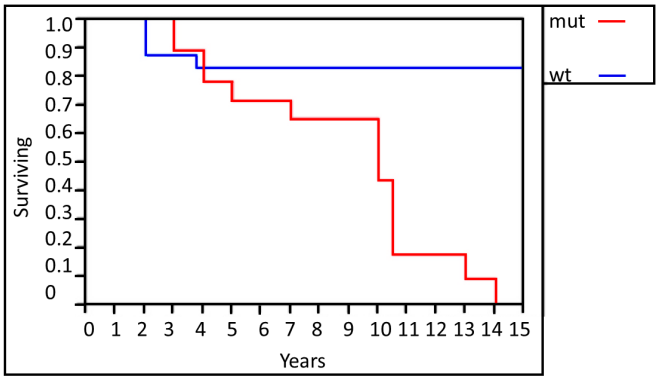

Figure 4. Disease-free estimator grouped by *TERT* mutation. The horizontal axis represents time in years, and the vertical axis shows the probability of surviving without recurrence. Abbreviations: Wt-wild-type *TERT*; mut-*TERT* promoter mutations C228T or C250T

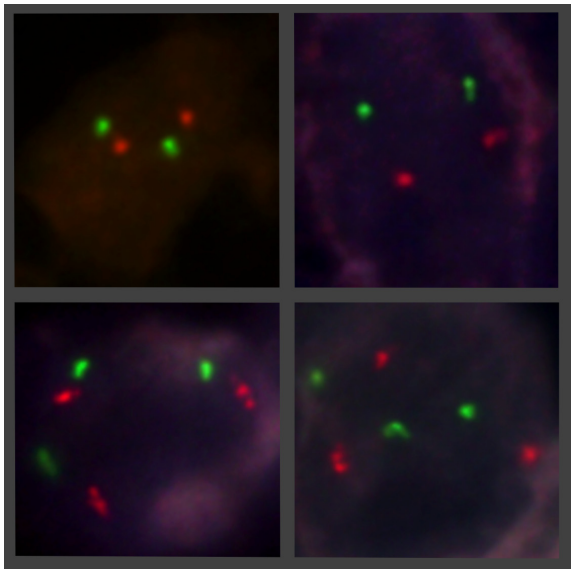

Figure 5. Detection of the copy numbers of *TERT* gene evaluated by: individual interphase nuclei; histological sections from formalin-fixed and paraffin-embedded tissues (four different SFT patients); ZytoLight SPEC TERT/5q31 dual-color probes mixture (*TERT* gene region 5p15.33 labeled with green fluorochrome; region 5q31.2 labeled with red fluorochrome). Notes: Upper row: two patients with 2 signals for *TERT* gene and 2 signals for 5q31; lower row: two patients with 3 signals for *TERT* gene and 3 signals for 5q31

Ki-67 mRNA expression. The median of *Ki-67* mRNA for benign SFT was 2.1×10^{-3}, the median of *Ki-67* mRNA for SFT with uncertain biological behavior was 8.3×10^{-3} and 2.26×10^{-2} for malignant SFTs. The mRNA expression correlated with local recurrences (p=0.0043) and biological behavior of the tumor (p=0.0270), but did not correlate with the type of the *NAB2/STAT6* fusion (p=0.1140). The level of *Ki-67* mRNA correlated with IHC established results (p=0.0270).

TPX2 mRNA expression. The median of *TPX2* mRNA for benign SFT was 2.9×10^{-2}, the median of *TPX2* mRNA for SFT with uncertain biological behavior was 6.8×10^{-2} and 2.01×10^{-1} for malignant SFTs.

The *TPX2* mRNA expression correlated with local recurrences (p=0.0190) and with biological behavior of the tumor (p=0.0390). The mRNA *TPX2* expression did not correlate with the type of the *NAB2/STAT6* fusion (p=0.4200). The mRNA *TPX2* expression correlated well with the mRNA expression of *Ki-67* (p<0.0001) and with the mRNA expression of *TERT* (p<0.0001).

TERT mRNA expression. The *TERT* mRNA expression for benign SFT was negative, the median of *TERT* mRNA for SFT with uncertain biological behavior was 4.65×10^{-3} and 4.54×10^{-3} for malignant SFTs.

The mRNA *TERT* expression correlated with local recurrences (p<0.0001, Figure 2), also correlated with the biological behavior of the tumor (p=0.0006). The majority of SFTs with benign behavior was without detectable expression of *TERT* mRNA. The mRNA *TERT* expression did not correlate with the type of the *NAB2/STAT6* fusion (p=0.4700) but correlated well with the mRNA expression of *Ki-67* (p<0.0001) and with the mRNA expression of *TPX2* (p<0.0001).

TERT promoter mutation. The *TERT* promoter mutation rate was 35% (22/63) in SFT patients and was associated with malignant (66.6%, 8/12) and uncertain (63%, 14/22) biological potential of SFTs. The data are summarized in OncoPlot (Figure 3).

Twenty-two patients with *TERT* promoter mutations harbored the C228T mutation and only one carried the C250T mutation. The disease-free survival estimator in SFT with and without *TERT* promoter mutation is displayed in Figure 4.

FISH. Fluorescence in situ hybridization analysis was performed in order to identify a possible role of the *TERT* gene amplification in the increased levels of *TERT* mRNA. In 6 cases with overexpressed *TERT* mRNA without *TERT* promoter mutation, FISH did not reveal amplification of the *TERT* gene (Figure 5). This finding suggests that *TERT* mRNA overexpression in SFTs is related to some other pathogenic mechanisms than gene amplification.

Discussion

SFTs are mesenchymal fibroblastic tumors with an unpredictable biological potential ranging from benign to malignant. Multiple approaches were developed to identify malig-

nant tumors; however, the criteria used to date fail to reliably predict the individual clinical course. In this retrospective single-institution study, we analyzed 74 samples (65 patients) of SFTs originating from the pleura and other extrapleural localizations and analyzed prognostic factors to predict recurrence and survival.

According to the newest criteria of the World Health Organization [1, 3], solitary fibrous tumor appears equally between sexes, males and females. In our study, 37 females and 28 males with SFT were evaluated: 8 females with malignant, 10 with uncertain, and 19 with benign biological behavior, 4 males with malignant, 12 with uncertain, and 12 with benign biological behavior.

The most beneficial markers for predicting biological behavior as published by Franzen and Schmid [4, 12] are the mitotic rate and proliferation index measured by Ki-67 expression.

In this study, we found significantly higher counts of mitosis per 10 HPF and Ki-67 index in SFTs with malignant behavior in comparison to uncertain or benign. These data are in concordance with the published study of Schmid or Yokoi [5, 12]. The number of mitotic figures per 10 HPFs and proliferation rate (measured with Ki-67 immunohistochemistry) correlated well ($p<0.0001$). Moreover, recurrent tumors displayed an increased Ki-67 labeling index in comparison to the primary tumors. This finding is consistent with the observation of Hiraoka et al. suggesting that SFTs might increase their malignant capacity with every recurrence [28].

Recently, Moghaddam et al. published a cut-off level of a proliferation rate of 12% Ki-67, which was proposed to indicate benign and malignant lesions [29]. The problem may be that this cut-off limit was set for adenocarcinomas vs. reactive mesothelial cells and different tumors may behave differently. Also, the assessment of Ki-67 immunoscore may suffer from inter- and intra-observer variability [4]. That is why we focused on the investigation of proliferation and telomerase activity of SFTs using RQ-RT-PCR to estimate their biological behavior with greater accuracy than establishing the mitotic rate and/or proliferation index. In the present study, we used data of RQ-RT-PCR that determines a real amount of the target molecules, expressed as a copy number of molecules. Proliferative marker Ki-67 antigen is the most common marker for the detection of the proliferation activity of tumors using IHC investigations. We observed a good correlation between *Ki-67* mRNA expression and Ki-67 protein expression using IHC ($p=0.0200$). We also found a statistical significance of *Ki-67* mRNA expression levels in the group of SFTs with benign behavior when compared with malignant and/or uncertain SFTs ($p=0.0091$). The comparison of benign SFTs vs. malignant was statistically significant ($p=0.0010$), but the comparison of benign vs. uncertain SFTs did not reach statistical significance probably because of the limited number of cases in each group ($p=0.1011$). The patients with recurrent tumors had significantly higher *Ki-67* mRNA levels than patients without recurrence ($p=0.0250$). Similarly, we found a statistical significance of *TPX2* mRNA expression levels in the group of SFTs with benign behavior when compared with malignant and/or uncertain SFTs ($p=0.0200$). TPX2 plays a key role in cell cycle promotion and mitotic division. TPX2 is expressed in the proliferating cells in S, G2, and M phases of the cell cycle and its activity corresponds to the proliferation activity of cells [18].

As the best molecular marker for distinguishing of biological behavior of SFTs seems to us the *TERT* mRNA expression level. Reactivation of telomerase activity is believed to play a role in tumor cell immortalization. We found a statistical significance of *TERT* mRNA expression levels in the group of SFTs with benign behavior when compared with malignant and/or uncertain SFTs ($p<0.0001$). So, we demonstrated the association of the *TERT* mRNA level and SFTs with malignant (median of expression 2.75e-3) or uncertain biological behavior (median of expression 8.29e-4) in comparison to benign SFTs without detectable mRNA expression of *TERT* (median of expression 0). The mRNA *TERT* expression correlated well with the mRNA expression of *Ki-67* ($p<0.0001$) and with the mRNA expression of *TPX2* ($p=0.0006$).

The *TERT* promoter mutation rate was 35% (22/63) in SFT patients and was associated with malignant (66.6%, 8/12) and uncertain (63%, 14/22) biological potential of SFTs. This finding is in correlation with published data of Demicco et al. [30], Park et al. [31], and Bahrami et al. [32].

In SFTs with overexpression of *TERT* mRNA but without promoter mutation, the FISH analysis confirmed that the high level of *TERT* mRNA in SFTs is not related to gene amplification but is most probably caused by alternative mechanisms such as methylation of the TERT Hypermethylated Oncological Region (THOR) or other mechanisms.

Recurrent fusion between the two genes *NAB2* and *STAT6*, both located at chromosomal region 12q13 have been identified by next-generation sequencing and RT-PCR in most SFTs [14, 33, 34]. This intrachromosomal inversion likely represents an initial tumorigenic event in SFTs.

All 65 patients with SFTs, which were immunohistochemically investigated, showed positivity of STAT6 protein. For the molecular analysis, we have had 74 samples from 65 patients. *NAB2-STAT6* fusion transcript was found in 63/74 cases (85%) of amplifiable samples and in 57/65 patients with SFT (87.7%). Fourteen different fusion variants were found in the 65 patients with SFTs. Five cases with good quality of RNA (all FFPE) had no detectable *NAB2-STAT6* fusion despite nuclear positivity for STAT6. We can speculate about the possibility that there are other gene fusions involved in a subgroup of SFTs. Furthermore, in single cases with other fusion genes have been reported, for example, *STAT6-TRAPPC5* [34], and probably additional fusion genes will be detected in the future. The other 3 cases with the negativity of the control housekeeping gene *ABL* were negative according to the technical limitation of the method. Most tumors with the fusion *NAB2* exon 4 and *STAT6* exon 2 were detected

in patients with pleuropulmonary localization. Similarly, tumors with the fusion *NAB2* exon 6 with the *STAT6* exon 16/17 were mainly deep-seated in the extremities and retroperitoneal or pelvic soft tissues. These data are in concordance with published data by Barthelmess et al. [33] and Vogels [9]. The fusion variants did not correlate with *Ki-67*, *TPX2,* and *TERT* mRNA levels. Also, certain translocation breakpoints for the *NAB2-STAT6* fusion gene have been associated with prognosis in SFT, the prognostic implication of fusion variants is still controversial [6, 33, 35].

In conclusion, using a combination of methods listed above, such as mitotic rate, proliferation activity settled by immunohistochemistry and mRNA expression, is helpful for the prediction of the tumor biological behavior. There is a good concordance between STAT6 immunostaining and *NAB2-STAT6* fusion transcripts in SFTs. It seems that STAT6 immunohistochemistry is a powerful diagnostic tool. Also, the identification of the *NAB2-STAT6* fusion gene can provide important diagnostic, but not prognostic information.

Detection of *TERT* mRNA expression at routine practice might lead to a better estimation of the biological potential of SFTs.

Finally, in the era of advocating minimally invasive needle biopsy for deep-seated mesenchymal tumors, it is highly desirable to have molecular testing to aid in the diagnosis of difficult cases and to predict the biological potential of SFTs from needle biopsies.

Supplementary information is available in the online version of the paper.

Acknowledgments: The authors acknowledge the financial support of the Research Project of the Ministry of Health No 00064203.

References

[1] DEMICCO EG, FRITCHIE KJ, HAN A. Solitary fibrous tumor. In WHO Classification of Tumours of Soft Tissue and Bone, 5th Edition. IARC, 2020, vol. 3. Lyon: International Agency for Research on Cancer (IARC), Lyon 2020. ISBN 928-32-4502-4

[2] EL-NAGGAR AK, RO JY, AYALA AG, WARD E, ORDONEZ NG. Localized fibrous tumor of the serosal cavities. Immunohistochemical, electron-microscopic, and flow-cytometric DNA study. Am J Clin Pathol 1989; 92: 561–565. https://doi.org/10.1093/ajcp/92.5.561

[3] FLETCHER GA, CHRISTOPHER DM. Solitary fibrous tumor. In WHO classification of Lung, Pleura, Thymus and Heart, 4 th Edition, IARC, Lyon 2015. ISBN 978-92-832-2436-5

[4] FRANZEN D, DIEBOLD M, SOLTERMANN A, SCHNEITER D, KESTENHOLZ P et al. Determinants of outcome of solitary fibrous tumors of the pleura: An observational cohort study. BMC Pulm Med 2014; 14: 138. https://doi.org/10.1186/1471-2466-14-138

[5] YOKOI T, TSUZUKI T, YATABE Y, SUZUKI M, KURUMAYA H et al., Solitary fibrous tumour: Significance of p53 and CD34 immunoreactivity in its malignant transformation. Histopathology 1998; 32: 423–432. https://doi.org/10.1046/j.1365-2559.1998.00412.x

[6] AKAIKE K, KURISAKI-ARAKAWA A, HARA K, SUEHARA Y, TAKAGI T et al. Distinct clinicopathological features of NAB2-STAT6 fusion gene variants in solitary fibrous tumor with emphasis on the acquisition of highly malignant potential. Hum Pathol 2015; 46: 347–356. https://doi.org/10.1016/j.humpath.2014.11.018

[7] YOSHIDA A, TSUTA K, OHNO M, YOSHIDA M, NARITA Y et al. STAT6 immunohistochemistry is helpful in the diagnosis of solitary fibrous tumors. Am J Surg Pathol 2014; 38: 552–559. https://doi.org/10.1097/PAS.0000000000000137

[8] DOYLE LA, VIVERO M, FLETCHER CDM, MERTENS F, HORNICK JL. Nuclear expression of STAT6 distinguishes solitary fibrous tumor from histologic mimics. Mod Pathol 2014; 27: 390–395. https://doi.org/10.1038/modpathol.2013.164

[9] VOGELS RJC, VLENTERIE M, VERSLEIJEN-JONKERS YMH, RUIJTER E, BEKERS EM et al. Solitary fibrous tumor – clinicopathologic, immunohistochemical and molecular analysis of 28 cases. Diagn Pathol 2014; 9: 224. https://doi.org/10.1186/s13000-014-0224-6

[10] YAN B, RAJU GC, SALTO-TELLEZ M. Epithelioid, cytokeratin expressing malignant solitary fibrous tumour of the pleura. Pathology 2008; 40: 98–99. https://doi.org/10.1080/00313020701716417

[11] CAVAZZA A, ROSSI G, AGOSTINI L, RONCELLA S, FERRO P et al. Cytokeratin-positive malignant solitary fibrous tumour of the pleura: An unusual pitfall in the diagnosis of pleural spindle cell neoplasms. Histopathology 2003; 43: 606–608. https://doi.org/10.1111/j.1365-2559.2003.01703.x

[12] Schmid S, Csanadi A, Kaifi JT, Kübler M, Haager B et al. Prognostic factors in solitary fibrous tumors of the pleura. J Surg Res 2015; 195: 580–587. https://doi.org/10.1016/j.jss.2015.01.049

[13] CHMIELECKI J, CRAGO AM, ROSENBERG M, O'CONNOR R, WALKER SR et al. Whole-exome sequencing identifies a recurrent NAB2-STAT6 fusion in solitary fibrous tumors. Nat Genet 2013; 45: 131–132. https://doi.org/10.1038/ng.2522

[14] ROBINSON DR, WU YM, KALYANA-SUNDARAM S, CAO X, LONIGRO RJ et al. Identification of recurrent NAB2-STAT6 gene fusions in solitary fibrous tumor by integrative sequencing. Nat Genet 2013; 45: 180–185. https://doi.org/10.1038/ng.2509

[15] Tai HC, Chuang IC, Chen TC, Li CF, Huang SC et al. NAB2-STAT6 fusion types account for clinicopathological variations in solitary fibrous tumors. Mod Pathol 2015; 28: 1324–1335. https://doi.org/10.1038/modpathol.2015.90

[16] DAS NEVES LRDO, OSHIMA CTF, ARTIGIANI-NETO R, YANAGUIBASHI G, LOURENÇO LG, FORONES NM. Ki67 and p53 in gastrointestinal stromal tumors – GIST. Arq Gastroenterol 2009; 46: 116–120. https://doi.org/10.1590/s0004-28032009000200008

[17] WARNER SL, STEPHENS BJ, NWOKENKWO S, HOSTETTER G, SUGENG A et al. Validation of TPX2 as a potential therapeutic target in pancreatic cancer cells. Clin Cancer Res 2009; 15: 6519–6528. https://doi.org/10.1158/1078-0432.CCR-09-0077

[18] KALFUSOVA A, HILSKA I, KRSKOVA L, KALINOVA M, LINKE Z et al. Gastrointestinal stromal tumors – Quantitative detection of the Ki-67, TPX2, TOP2A, and hTERT telomerase subunit mRNA levels to determine proliferation activity and a potential for aggressive biological behavior. Neoplasma 2016; 63: 484–492. https://doi.org/10.4149/320_150714N390

[19] RK MOYZIS, BUCKINGHAM JM, CRAM LS, DANI M, DEAVEN LL et al. A highly conserved repetitive DNA sequence, (TTAGGG)(n), present at the telomeres of human chromosomes. Proc Natl Acad Sci USA 1988; 85: 6622–6626. https://doi.org/10.1073/pnas.85.18.6622

[20] BLACKBURN EH. Structure and function of telomeres. Nature 1991; 350: 569–573. https://doi.org/10.1038/350569a0

[21] NW KIM, PIATYSZEK MA, PROWSE KR, HARLEY CB, WEST MD et al. Specific association of human telomerase activity with immortal cells and cancer. Science 1994; 266: 2011–2015. https://doi.org/10.1126/science.7605428

[22] BROCCOLI D, YOUNG JW, DE LANGE T. Telomerase activity in normal and malignant hematopoietic cells. Proc Natl Acad Sci USA 1995; 92: 9082–9086. https://doi.org/10.1073/pnas.92.20.9082

[23] LIU L, LAI S, ANDREWS LG, TOLLEFSBOL TO. Genetic and epigenetic modulation of telomerase activity in development and disease. Gene 2004; 340: 1–10. https://doi.org/10.1016/j.gene.2004.06.011

[24] NAKAMURA TM, MORIN GB, CHAPMAN KB, WEINRICH SL, ANDREWS WH et al. Telomerase catalytic subunit homologs from fission yeast and human. Science 1997; 277: 955–959. https://doi.org/10.1126/science.277.5328.955

[25] T SAITO, AKAIKE K, KURISAKI-ARAKAWA A, TODA-ISHII M, MUKAIHARA K et al. TERT promoter mutations are rare in bone and soft tissue sarcomas of Japanese patients. Mol Clin Oncol 2016; 4: 61–64. https://doi.org/10.3892/mco.2015.674

[26] LEÃO R, LEE D, FIGUEIREDO A, HERMANNS T, WILD P et al. Combined genetic and epigenetic alterations of the TERT promoter affect clinical and biological behavior of bladder cancer. Int J Cancer 2019; 144: 1676–1684. https://doi.org/10.1002/ijc.31935

[27] BIJWAARD KE, AGUILERA NSI, MONCZAK Y, TRUDEL M, TAUBENBERGER JK et al. Quantitative real-time reverse transcription-PCR assay for cyclin D1 expression: Utility in the diagnosis of mantle cell lymphoma. Clin Chem 2001; 47: 195–201.

[28] HIRAOKA K, MORIKAWA T, OHBUCHI T, KATOH H. Solitary fibrous tumors of the pleura: Clinicopathological and immunohistochemical examination. Interact Cardiovasc Thorac Surg 2003; 2: 61–64. https://doi.org/10.1016/S1569-9293(02)00091-9

[29] MOGHADDAM N, TAHERI D, RAHMANI A, DESFULI M. Proliferative index using Ki-67 index in reactive mesothelial versus metastatic adenocarcinoma cells in serous fluid. Adv Biomed Res 2012; 1: 29. https://doi.org/10.4103/2277-9175.98155

[30] DEMICCO EG, WANI K, INGRAM D, WAGNER M, MAKI RG et al. TERT promoter mutations in solitary fibrous tumour. Histopathology 2018; 73: 843–851. https://doi.org/10.1111/his.13703

[31] PARK HK, YU DB, SUNG M, OH E, KIM M et al. Molecular changes in solitary fibrous tumor progression. J Mol Med (Berl) 2019; 97: 1413–1425. https://doi.org/10.1007/s00109-019-01815-8

[32] BAHRAMI A, LEE S, SCHAEFER IM, BOLAND JM, PATTON KT et al. TERT promoter mutations and prognosis in solitary fibrous tumor. Mod Pathol 2016; 29: 1511–1522. https://doi.org/10.1038/modpathol.2016.126

[33] BARTHELMESS S, GEDDERT H, BOLTZE C, MOSKALEV EA, BIEG M et al. Solitary fibrous tumors/hemangiopericytomas with different variants of the NAB2-STAT6 gene fusion are characterized by specific histomorphology and distinct clinicopathological features. Am J Pathol 2014; 184: 1209–1218. https://doi.org/10.1016/j.ajpath.2013.12.016

[34] MOHAJERI A, TAYEBWA J, COLLIN A, NILSSON J, MAGNUSSO L et al. Comprehensive genetic analysis identifies a pathognomonic NAB2/STAT6 fusion gene, nonrandom secondary genomic imbalances, and a characteristic gene expression profile in solitary fibrous tumor. Genes Chromosomes Cancer 2013; 52: 873–886. https://doi.org/10.1002/gcc.22083

[35] KOELSCHE C, SCHWEIZER L, RENNER M, WARTH A, JONES DTW et al. Nuclear relocation of STAT6 reliably predicts NAB2-STAT6 fusion for the diagnosis of solitary fibrous tumour. Histopathology 2014; 65: 613–622. https://doi.org/10.1111/his.12431

https://doi.org/10.4149/neo_2021_210511N642

Determination of biological behavior of solitary fibrous tumors: correlation of expression of *Ki-67*, *TPX2* and *TERT* mRNA subunit level and *NAB2-STAT6* fusion compared to morphological aspects of SFTs

Lenka KRSKOVÁ[1,*], Igor ODINTSOV[1,2], Ondřej FABIÁN[1,3,4], Petra HROUDOVÁ[1,5], Marcela MRHALOVÁ[1]

Supplementary Information

Supplementary Table S1. List of primary antibodies used for immunohistochemical study of SFTs.

Primary antibody	Brand	Clone	Dilution	pH
CD34	Biogenex	QBend/10	1:30	6
BCL2	Dako	Clone 124	1:100	9
CD99	Neo Markers	O13	1:500	9
STAT6	Abcam	YE361	1:500	9
Ki-67	Dako	MIB-1	1:150	6

Supplementary Table S2. The list of primers.

	5´–3´seqences	Author
NAB2 ex3	CAAGTAGCCCGAGAGAGCAC	Vogels et al. 2014
NAB2 ex4	CTCCACTGAAGAAGCTGAAAC	
STAT6 ex2	GGGAAAGTCGACATAGAGCC	
NAB2 ex6	CTGTGTGCCTGCGAAGCC	
STAT6 ex17	GAGCTGAGCAAGATCCCGG	
STAT6 ex18	TTCCACGGTCATCTTGATGG	
NAB2 ex6S1	TATGGAGCCGACACATCCTG	Nakada et al. 2015
STAT6 ex16AS1	GCTGAGCAAGATCCCGGATT	
NAB2 ex6S2	CACATCCTGCAGCAGACACT	
STAT6 ex16AS2	AGCCTCATCCTTGGGCTTCT	
NAB2 ex5	CCTGTCTGGGGAGAGTCTGGATG	Robinson et al. 2013
STAT6 ex20	GGGGGGATGGAGTGAGAGTGTG	
NAB2 ex2	GGGGGGATGGAGTGAGAGTGTG	Tai et al. 2015
STAT6 ex19	GGGATGGAGTGAGAGTGTGG	
RQ-RT PCR		
Ki-67 F	GAGGTGTGCAGAAAATCCAAA	
Ki-67 R	CTGTCCCTATGACTTCTGGTTGT	
Ki-67 probe	Universal Probe Library, probe No 30[a]	
TPX2 F	ACATCTGAACTACGAAAGCATCC	
TPX2 R	GGCTTAACAATGGTACATCCCTTA	
TPX2 probe	Universal Probe Library, probe No 76[a]	
hTERT F	GCCTTCAAGAGCCACGTC	
hTERT R	CCACGAACTGTCGCATGT	
hTERT probe	Universal Probe Library, No19[a]	

Note: [a]Roche Applied Science

Supplementary Table S3.

NAB2-STAT6 fusion variant	Number of cases
4 - 2	33
5 or 6 - 16,17,18	14
5 - 2	1
3 - 19	2
3 - 18	1
3 - 3	1
6 - 3	1
7 - 16	1
2 - 2	1
Intron 2-3 - 19	1
7-2	1